Desalination and Water Treatment
www.deswater.com

doi: 10.1080/19443994.2013.769757

51 (2013) 4666–4674
June

Taylor & Francis
Taylor & Francis Group

Pb^{2+} adsorption behavior of calix[4]arene based Merrifield Resin

Ashfaque Ali Bhatti, Asif Ali Bhatti, Imam Bakhsh Solangi, Shahabuddin Memon*

National Center of Excellence in Analytical Chemistry, University of Sindh, Jamshoro 76080, Pakistan
Tel. +92 (22) 9213430; Fax: +92 (22) 9213431; email: shahabuddinmemon@yahoo.com

Received 10 April 2012; Accepted 12 November 2012

ABSTRACT

The present study reveals the adsorption of heavy metals, especially Pb^{2+} from aqueous media by *p*-tetrathioureacalix[4]arene based Merrifield resin (**1**). The adsorption behavior of toxic Pb^{2+} metal was evaluated through batch experiments and various parameters such as dosage, concentration and temperature were optimized. From the kinetic study, it has been noticed that adsorption mechanism follows pseudo-second order kinetic model. In addition, thermodynamic constants of adsorption phenomena for Pb^{2+} was found to be ΔH = 0.098 kJ/mol and ΔS = 0.339 kJ/mol, the positive value of ΔH suggest endothermic nature and spontaneity of process estimated by negative value of ΔG. The experimental data was carried out by applying different isotherm equations such as Freundlich, Langmuir, and Dubinin–Radushkevich, (D–R). From the analysis it could be clearly understood that Pb^{2+} has been adsorbed chemically onto the surface of resin (**1**).In this view, calix[4]arene based resin (**1**) is very potential in minimize the risk of environmental water pollution by Pb^{2+}.

Keywords: Calix[4]arene; Merrifield resin; Adsorption; Isotherm equations; Kinetic study

1. Introduction

Recently, it has become prime important and challengeable task to control the environmental pollution. The presence of various toxicants such as transition/heavy metal ions, radionuclides and synthetic chemicals in groundwater, surface water and industrial effluents contribute toxic and deadly affect on the ecosystem [1]. Pollution due to heavy metal ions from anthropogenic and natural sources has got considerable importance because of their incapability to undergo biological degradation and cause many adverse effects to all living organisms by entering into the food chain and accumulating in various tissues [2]. The technological advancement and enhancement of industrial activities are the main factors, which bring about environmental contamination [3]. Among these toxicants, lead (Pb^{2+}) has significant hazardous effects not only to humans but also aquatic environment. The major sources of Pb^{2+} contamination in the environment are industrial effluents that are smelters, electroplating, metal refineries, textile, mining, tanneries, oil refineries, ceramic and glass industries [4–7]. The WHO permissible limit for Pb^{2+} in drinking water is 0.01 mg/L [8]. However, the excessive Pb^{2+} exposure may cause brain damage and dysfunction of kidneys, liver, and central nervous system in humans, headache, convulsions, behavioral disorders, and constipation and potentially can cause cancer from a lifetime exposure above the action level [9,10]. Therefore, the scientists have engaged in boosting up the techniques for the removal of Pb^{2+} from the drinking water. Many conventional methods have been

*Corresponding author.

adopted for the removal of toxic metal ions including chemical precipitation, coagulation/flocculation, ion exchange, solvent extraction, cementation, complexation, electrochemical operations, biological operations, evaporation, filtration, adsorption and membrane processes [11–15]. Among all these methods, adsorption has got significant advantages such as cost effectiveness, simple operation and environmental friendly approach [16,17]. A large number of adsorptive materials have been reported for the adsorption of heavy metals such as modified silica gel [18,19] activated carbon [20] biomaterials [21] inorganic materials [22] polymers [23]. Instead of all, calixarenes have got much attention in last few decades.

Calix[*n*]arenes are synthetic macrocyclic condensate products of phenol and formaldehyde obtained under alkaline medium. In the field of supramolecular systems they are considered as key receptors and have drawn tremendous attention for last three decades [24,25]. Due to their enormous applications, they have motivated scientists by synthesizing variety of derivatives; this can be done by incorporating different functionalities either at hydrophilic phenolic group or inserting at hydrophobic site, these molecules possess flexibility, different shapes and conformations [26,27]. Moreover, due to their three dimensional structure and fascinating characteristics they have motivated the development of useful methods resulting in the form of polymeric matrices, membranes, ion selective electrodes, sensors for chemical and biochemical processes and ionophores for selective extraction of toxic heavy metal ions [28–32].

The sensitivity and selectivity of calixarenes toward metal ions could be enhanced by the introduction of specific functional groups such as amide, carbonyl and nitrile along with their incorporation into polymeric material [33–37]. Besides this, calix[*n*]arene derivatives comprising of ester functionality have been proved as excellent extractants for Pb^{2+} ions [14,38–39]. While others containing sulfur, nitrogen in thiolates, thioether, dithiocarbamates, urea and substituted thiourea functionalities show extracting ability toward transition and precious metals [40,41]. The present work is an extension of our previous study [42] Thus; herein we report the application of *p*-tetrathioureacalix[4]arene based Merrifield resin (Fig. 1) containing sulfur and nitrogen binding sites to evaluate their adsorption behavior toward heavy metals.

2. Experimental

2.1. Apparatus

Melting points were determined on a Gallenkamp melting point apparatus model (MFB. 595.010M,

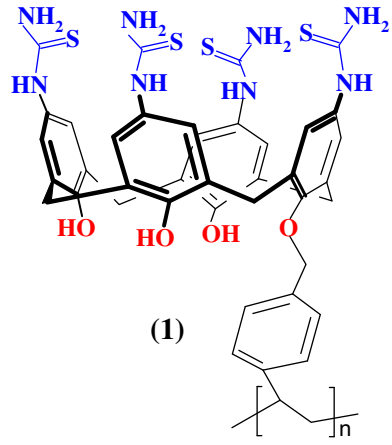

Fig. 1. Chemical structure of *p*-tetrathioureacalix[4]arene based Merrifield resin (**1**).

England) in a sealed capillary tube. IR spectra were recorded on a Thermo Nicollet 5700 FT-IR spectrometer (WI. 53711, USA) as KBr pellets. Elemental analyses were performed using a CHNS instrument (model Flash EA 1112, 20090-Rodano, Milan, Italy) elemental analyzer. A Gallenkamp thermostat automatic mechanical shaker model (BKS 305-101, UK) was used for batch study. UV/vis spectra were recorded on a PerkinElmer (Shelton, CT 06484, USA) Lambda 35 through UV/vis spectrophotometer.

2.2. Reagents

Analytical TLC was done on precoated silica gel plates (SiO_2, Merck PF_{254}, Darmstadt, Germany), silica gel with 60 (Merck, particle size 0.040-0.063mm, 230-400 mesh). Merrifield resin was purchased from Alfa Aesar (Germany). It is 1% cross linked having 200–400 mesh size and 1.0–1.3 mmol Cl/g resin as quoted by the supplier.

2.3. Adsorption procedure

2.3.1. Batch method

Batch wise experimental method was applied carried out for the adsorption of metal-picrates at room temperature, i.e. 30 ± 1°C, to investigate the affect of diverse parameters such as dosage, contact time, concentration and different temperatures on the adsorption of metal-picrate by calix[4]arene based Merrifield adsorbent material (**1**).

The experiments were performed in Erlenmeyer flasks containing (10 mL) sample solution of (5×10^{-5} mol/L) metal-picrate was placed in a mechanical shaker operating at a constant speed of

160 rpm. The resin after extraction was filtered off and the adsorption of metal-picrate was analyzed by using UV–Vis spectrophotometer. Adsorption of metal-picrate was calculated as follows;

$$\% \text{ adsorption} = \frac{C_i - C_f}{C_i} \times 100 \quad (1)$$

where C_i and C_f (mol/L) are the initial and final concentrations of solutions before and after the adsorption of different metal-picrates, respectively.

Metal-picrates of transition elements were prepared by stepwise mixing of a 1×10^{-2} M of metal nitrate solution to a flask containing 2.5×10^{-5} M aqueous solution of picric acid, after addition mixture was shaken for 1hour at 25°C [43].

3. Results and discussion

3.1. Adsorption studies

The adsorption efficiency of resin (**1**) was studied by solid-liquid extraction experiments. The adsorption experiment was performed with transition metal-picrates such as Hg^{2+}, Pb^{2+}, Cu^{2+}, Co^{2+}, Cd^{2+} and Ni^{2+} from aqueous media. The results are summarized in fig 2. It is interesting to note, that the order of the adsorption of metal cations by resin (**1**) decreases in the sequence of $Pb^{2+} > Hg^{2+} > Cu^{2+} > Cd^{2+} > Co^{2+} > Ni^{2+}$.

3.1.1. Effect of adsorbent dosage

Adsorbent dosage is a significant parameter used to evaluate the adsorbent capacity for adsorbate of known concentration at operating conditions. The effect of resin on the % removal of Pb^{2+} was investigated by varying the dosage of resin at a fixed concentration of Pb^{2+}-picrate. The percent (%) adsorption of Pb^{2+}-picrate enhanced by increasing the dosage of resin (**1**) and the adsorption at higher dosage than 0.1 g were remained almost constant (Fig. 3). This was

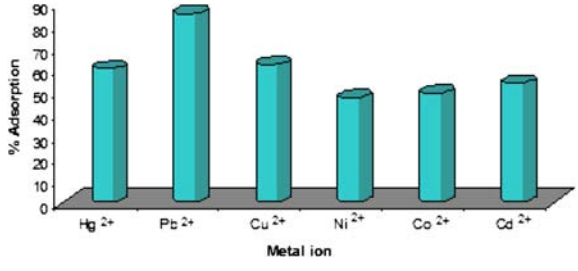

Fig. 2. Percent adsorption of different metal picrates, (10 mL of metal picrate concentration 2.5×10^{-5}, 60 min contact time).

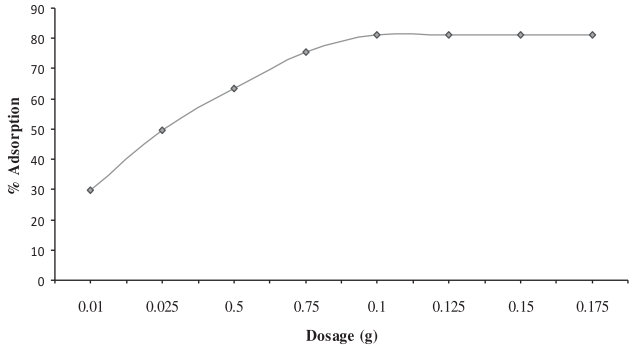

Fig. 3. Effect of adsorbent dosage on the percent adsorption of Pb^{2+} (10 mL of Pb^{2+} picrate, concentration 2.5×10^{-5}, 60 min contact time).

for the reason of that the availability of excessive adsorbate surface for the solute to be adsorbed.

3.1.2. Optimum shaking time

For the evaluation of affect of shaking time on the adsorption of Pb^{2+}-picrate on resin (**1**) was studied at different temperatures ranges (303–313 K). It was concluded from figure (6) that with the rise of shaking time and temperature the percent adsorption of Pb^{2+}-picrate onto resin (**1**) also increases; this indicates Pb^{2+} adsorbed onto the surface of resin (**1**) is endothermic in nature. The adsorption was rapid during the first 15 min at different temperatures then increases slightly up to 30 min and equilibrium was attained. On the basis of results, for maximum adsorption 30 min shaking time was found suitable and the equilibrium was obtained within this time period.

3.1.3. Comparison of Pb^{2+}-picrate adsorption with other adsorbents

The maximum adsorption capacity of resin (**1**) for Pb^{2+}-picrate at pH 6.5 and 35°C has been evaluated as 84.80 mmol/g. A comparison of maximum Pb^{2+}-picrate adsorption capacity *qm* of resin (**1**) with other adsorbents reported in literature [44–51] is given in (Table 1). The data show that the adsorption capacity of resin (**1**) is relatively high when compared with other reported adsorbent materials.

3.2. Adsorption kinetics of Pb^{2+}- picrate.

The adsorption kinetics study depicts the uptake rate of solute, and at the solid/solution interface this rate obviously controls the residence time of adsorbate uptake, including the diffusion process. Besides this, the adsorption mechanism depends on the physical

Table 1
Comparison of adsorption performance of resin (**1**) with others

Name of adsorbent	pH	T (℃)	q_m	k_L	References
Bamboo dust		30	5.950 mg/g	1.33 L/mg	Kannan and Veemraj [44]
Commercial activated carbon		30	2.151 mg/g	0.569 L/mg	Kannan and Veemraj [44]
Amberlite XAD-2 functionalized with Tiron	4–6		12.60 mg/g		Kumar et al. [45]
Grinded EucalyptusStem			4.49 mg/g	0.065 L/mg	Mousavi et al. [46]
Leavesof Date Trees	5	25	55.56 mg/g	0.353 mg/g	Boudrahem et al. [47]
GNS			22.42 mg/g	65.01 L/mg	Huang et al. [48]
GNS500			35.21 mg/g	414.74 L/mg	Huang et al. [48]
Cashew nut shells A.C.	6.0–6.5	30	28.90 mg/g	0.0029 L/mg	Tangjuank et al. [49]
Hazelnut husk A.C.	5.7		13.05 mg/g		Immamuglu et al. [50]
MWCNTs	6.0	20	33.0 mg/g	2.03 L/mg	Xiaowei Zhao et al. [51]
Resin (**1**)		30	84.80 mmol/g	6.22×10^4 mol/L	This study

and chemical characteristics of the adsorbent as well as on the mass transfer process. Adsorption capacity of resin (**1**) for Pb^{2+} in terms of kinetic approach was evaluated as shown in (Fig. 5), plot of q_t vs. t at 303–313 K. In order to verify the mechanism of adsorption process by applying Kinetic models i.e. Lagergren pseudo-first-order and pseudo-second-order rate laws. From these results It has been concluded that the rate of Pb^{2+}-picrate adsorption onto resin (**1**) at 303–313 K tends to follow both pseudo-first-order and pseudo second-order rate Eqs. (2) and (3) [52]; as given under.

$$\ln(q_e - q_t) = \ln q_e - k_1 t \tag{2}$$

where q_t, q_e is the amount of Pb^{2+}-picrate (mol/ g) adsorbed at time t, and at equilibrium respectively, and k_1 (L/min) is the pseudo-first-order rate constant and its values were obtained from slopes and intercept of the linear plot. In Table 1, the k_1 values are listed for the adsorption of Pb^{2+}-picrate onto resin (**1**) which was determined at 303–313 K. On the other hand, the adsorption kinetics may be described by pseudo-second order [53]. The pseudo-second-order equation is also based on the adsorption capacity of the solid phase and is expressed as;

$$\frac{dq}{dt} = k_2(q_e - q_t)^2 \tag{3}$$

where k_2 is the rate constant of second-order adsorption. For the same boundary conditions the integrated form of Eq. (3) written as in Eq. (4).

$$\frac{t}{q_t} = \left(\frac{t}{k_2 q_e^2}\right) + \left(\frac{1}{q_e}\right) \tag{4}$$

For the second-order kinetics equation applicability can be judged by plotting t/q against t of Eq. (4) should have a linear relationship, from the slope and intercept of plot, the values of q_e and k_2 can be calculated, as are listed in Table 2.

It can be observed that the pseudo-second-order model fit the experimental data significantly well and provides better correlation coefficients than the pseudo- first-order model for resin (1). On contrary to the pseudo-first-order equation, pseudo-second-order equation fitting well to the kinetic experimental data and showed excellent linearity with high correlation coefficient (R^2 = 0.99) over different ranges of temperature, i.e 303–313 K.

In an adsorption process, the adsorbate molecules are most probably transported from the bulk of the solution into the solid phase through intraparticle/ film diffusion transport. So from kinetic models, Reichenberg equation was applied to make sure either the adsorption process of Pb^{2+}-picrate onto resin (**1**)

Table 2
Comparison of pseudo-first order and pseudo-second order kinetic model

Pseudo-first order kinetic model			Pseudo-second order kinetic model		
K_1(min^{-1})	q_e (mol/g)	R^2	K_2 (min^{-1})	q_e (g/mol min^{-1})	R^2
0.15	2.43	0.86	1.93×10^{-15}	1.75×10^{-5}	0.99

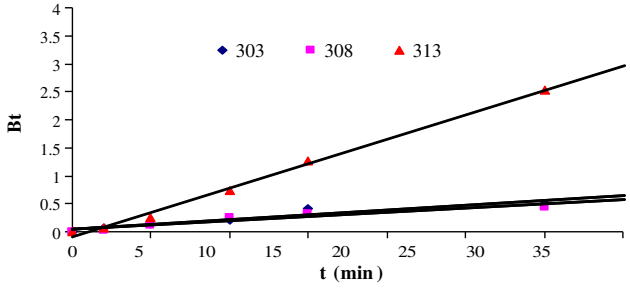

Fig. 4. Reichenberg (R–B) plot for the adsorption of Pb^{2+}-picrate onto resin (**1**).

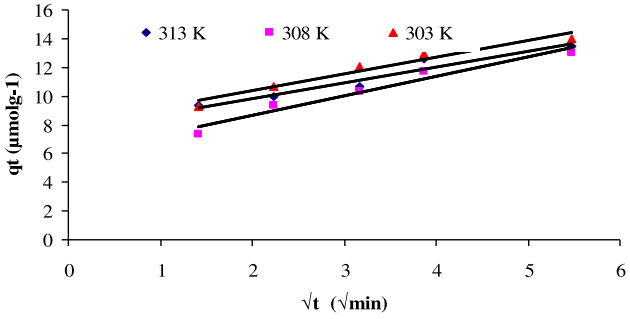

Fig. 5. Morris-Weber plot for the adsorption of Pb^{2+}-picrate onto resin (**1**).

takes place via film diffusion or intraparticle mechanism [54]. The equation written as:

$$Q = 1 - \frac{6e^{-B_t}}{\pi^2} \tag{5}$$

where $Q = q_t/q_e$, $B_t = \pi^2 D_i / r^2$, q_t and q_e are adsorbed concentration at time t and the maximum adsorption capacity respectively, D_i is the effective diffusion coefficient of the adsorbate inside the adsorbate particle. B_t which is the mathematical function of Q, which can be calculated for each value by sing following equation:

$$B_t = -0.4977 - \ln(1 - Q) \tag{6}$$

Plot of B_t vs. time t in figure, follow linearity and was employed to differentiate the external transport-(film diffusion) and intraparticle-transport-controlled rates of adsorption. A straight line passing through the origin which clearly exhibits intraparticle approach and a small friction of adsorption that occurs through this mechanism (Fig. 4).

Examination of kinetic adsorption was also performed by applying Morris–Weber equation [55];

$$q_t = R_d\sqrt{t} \tag{7}$$

where q_t is adsorbed concentration at time t, and R_d is the rate constant of intra particle transport. Plot of q_t (mol/ g) vs. $\sqrt{t}$ in Fig. 5 shows linearity in graph, From the slope in the initial stage the value of R_d and the rate constant of intraparticle transport is calculated to be as 1.103 µmol/g $t^{-1/2}$ (303 K), 1.364 µmol/g $t^{-1/2}$ (308 K) and 1.1649 µmol/g $t^{-1/2}$ (313 K) with R^2 values 0.921, 0.905 and 0.995 respectively.

3.3. Thermodynamics of adsorption

Temperature is another important criterion and definitely plays a key role in adsorption studies. So for the interpretation of percent adsorption of Pb^{2+}-picrate onto resin (**1**) as a function of temperature, adsorption studies were performed at different temperatures (i.e. from 303 to 313 K) to determine the thermodynamic parameters (Fig. 6).

These thermodynamic parameters such as Gibbs free energy (ΔG), enthalpy (ΔH) and entropy (ΔS) were calculated by the following Eqs. (8) and (9) are shown in Table 3.

$$\Delta G = -RT \ln k_c \tag{8}$$

Enthalpy ΔH and entropy ΔS of adsorption can be predicted from Van't Hoff Eq. (3).

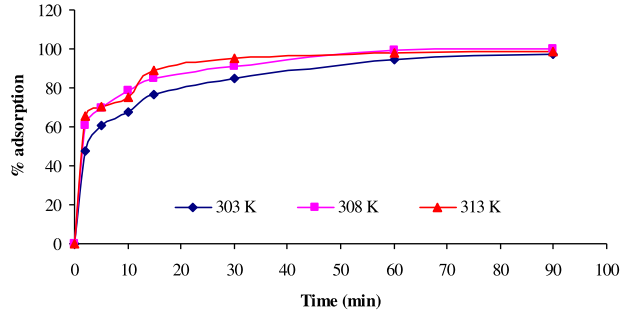

Fig. 6. Adsorption curve of Pb^{2+}-picrate onto resin (**1**) as function of time at different temperatures.

Table 3
Thermodynamic parameters for adsorption of Pb^{2+}-picrate onto resin (**1**)

ΔH (kJ/ mol)	ΔS (kJ/mol/ K)	ΔG (kJ/mol)		
		303 K	308 K	313 K
0.098	0.339	−7.721	−5.992	−4.333
		$\ln K_c = 1.720$	$\ln K_c = 2.341$	$\ln K_c = 2.968$

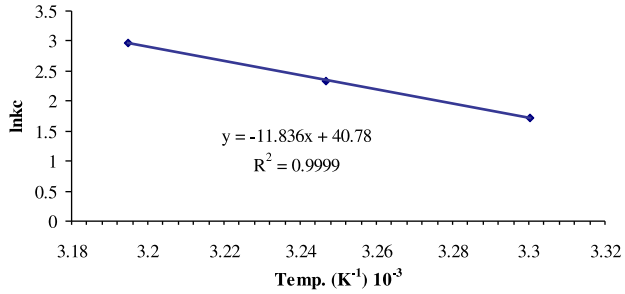

Fig. 7. Effect of Temperature on the adsorption of Pb^{2+}-picrate onto resin (**1**).

$$\ln k_c = \frac{-\Delta H}{RT} + \frac{\Delta S}{R} \tag{9}$$

where R (8.314 J/mol K) is the gas constant, k_c is adsorption equilibrium constant. The values of Gibbs free energy ΔG^0 were calculated from equation 8. Values of ΔS^0 and ΔH^0 can be obtained from the plot of ln k_c vs. $1/T$ (Fig. 7) using Eq. (9).

From the values of these two parameters, ΔG^0 was determined from Eq. (8) was found as −7.72, −5.99 and −4.33 (kJ/mol) at $T = 303$, 308, and 313 K respectively .The negative values of ΔG^0 confirms spontaneity and feasibility of Pb^{2+}-picrate adsorption onto resin (**1**), whereas, from the slope and intercept of the plot of ΔG^0 vs. T, the values of ΔH^0 and ΔS^0 were determined. ΔH^0 was figure out as 0.098 kJ/mol and the value of ΔS^0 calculated 0.339 J/mol K^{-1}. Positive value of ΔH implies that the adsorption of Pb^{2+}-picrate is endothermic in nature. With the rise of temperature, value of ln k_c also increases; improved intraparticle rate of diffusion of the adsorbate might be responsible for this enhanced value. Moreover diffusion is an endothermic process increase in randomness at the solid/solution interface may be due to slightly positive value of ΔS^0 [56–58] and resin (**1**) shows significant affinity to Pb^{2+}-picrate.

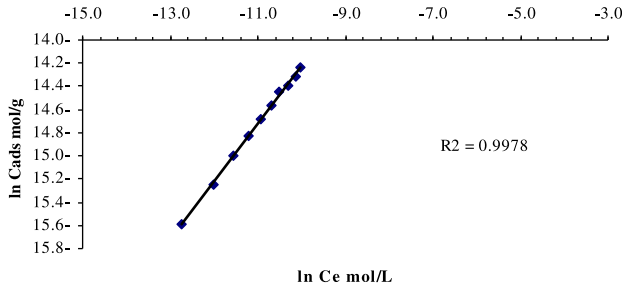

Fig. 8. Freundlich isotherm (Conc. 2.5×10^{-5} to 2.5×10^{-11} mol/L, 0.1 g adsorbent per 10 mL of adsorbate with 60 min shaking time at 30 ℃).

3.4. Adsorption isotherm

At a constant temperature, the adsorption isotherms are used to testify the relationship between the equilibrium concentrations of adsorbate in the aqueous phase and on the solid surface. Experimental data were used to evaluate the applicability of adsorption isotherms models, such as Langmuir, Freundlich and Dubinin–Radushkevich (D–R). These isotherm models were applied to compare the different parameters. The Freundlich isotherm was applied for the removal of Pb^{2+}-picrate by adsorption. Empirically this isotherm model based on equilibrium relationship at heterogeneous surfaces through multilayer adsorption, adsorption energy exponentially decreases on saturation of adsorptive sites of an adsorbent. The linearized form of Freundlich isotherm can be written as follow:

$$\ln C_{ads} = \ln A + \frac{1}{n} \ln C_e \tag{10}$$

where C_{ads} (mol/g) is the amount of Pb^{2+}-picrate adsorbed on the surface of adsorbent and C_e (mol/L) is the amount of Pb^{2+}-picrate in liquid phase at equilibrium. Freundlich isotherm constant adsorption capacity is A and $1/n$ is energy or adsorption intensity. The ln C_{ads} was plotted against ln C_e yielding a straight line (Fig. 8). From the straight line the value of slope obtained i.e. $1/n = 0.248$ and the value of intercept results $A = 101.98$ mg/g with a correlation factor $R^2 = 0.99$.

As Langmuir adsorption model covers monolayer adsorption and assumes all sites are equal in affinity to adsorbate as the energy of adsorption is constant and there is no migration of adsorbate molecules in the surface plane. Linear form of langmuir isotherm equation was applied for the evaluation of Pb^{2+}-picrate adsorption, can be represented in following form:

$$\frac{C_e}{C_{ads}} = \frac{1}{Qb} + \frac{C_e}{Q} \tag{11}$$

where C_e (mol/L) is the equilibrium concentration of in solution and C_{ads} (mol/g) is the amount of Pb^{2+}-picrate on adsorbent surface, Q is the maximum amount of solute adsorbed which imply the monolayer coverage of adsorbent surface, and b is a Langmuir constant relates about binding energy of solute. The plot of C_e/C_{ads} vs. C_e gives a straight line, which indicates the adsorption data follow Langmuir adsorption model very well. From the slope and intercept of Langmuir plot shown in Fig. 9, the values constant

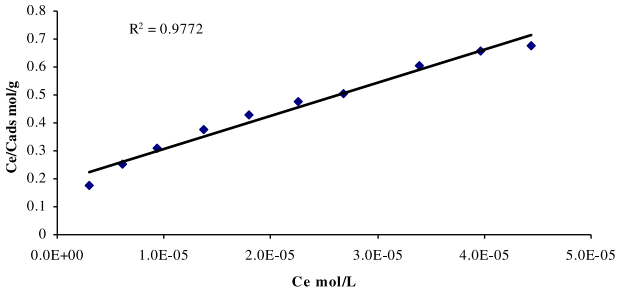

Fig. 9. Langmuir isotherm(Conc. 2.5×10^{-5} to 2.5×10^{-11} mol/L, 0.1 g adsorbent per 10 mL of adsorbate with 60 min shaking time at 30 ℃).

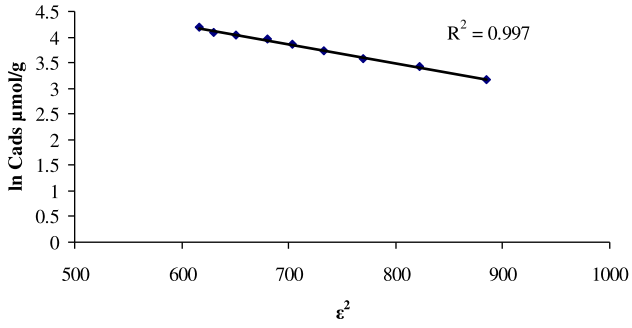

Fig. 10. D–R isotherm (Conc. 2.5×10^{-5} to 2.5×10^{-11} mol/L, 0.1 g adsorbent per 10 mL of adsorbate with 60 min shaking time at 30 ℃).

were evaluated as $Q = 204.08$ mg/g and $b = 0.925$ L/mg respectively. Characteristically, the isotherm shape of the Langmuir plot is used to predict the favorability of an adsorption system, it can be expressed in terms of equilibrium/separation parameter i.e R_L a dimensionless constant, which can be determined from following relation.

$$R_L = \frac{1}{(1 + bC_i)} \tag{12}$$

where b is the Langmuir constant (L/mg) and C_i is the initial concentration of Pb^{2+}-picrate (mol/L). The values of R_L indicate the shape of isotherm, such as,

$R_L > 1$ unfavorable
$R_L = 1$ linear
$R_L < 1$ and >0 favorable
$R_L = 0$ irreversible

From table the calculated value is 0.04–0.13, which represents Pb^{2+}-picrate adsorbed favorably onto resin (**1**).

The Dubinin–Radushkevich isotherm is applied to find the adsorption mechanism based on the potential theory assuming a heterogeneous surface. The Dubinin–Radushkevich (D–R) isotherm is more generally assume determine the adsorption heterogeneity of energies over the surface. The linear form of the D–R isotherm written as;

$$\ln C_{ads} = \ln X_m - \beta\varepsilon^2 \tag{13}$$

X_m is the total adsorption capacity; β is the activity coefficient, having dimensions of energy, and ε is the Polanyi potential, which is equal to

$$\varepsilon = RT \ln\left(1 + \frac{1}{C_e}\right) \tag{14}$$

where R is the gas constant (8.314 J/mol K) and T is the absolute temperature. The constant β gives the mean free energy, E of adsorption per molecule of the adsorbate when it is transferred to the surface of adsorbent. That means energy of adsorption, E (kJ/mol K^{-1}) can be calculated as

$$E = \frac{1}{\sqrt{-2\beta}} \tag{15}$$

A plot of ln C_{ads} vs. ε^2 gives straight line with slope β and intercepts X_m (Fig. 10).

On the basis of correlation coefficients (R^2) values as in (Table 4), it was deduced that adsorption phenomenon follow all three models i.e. Langmuir, Freundlich and Dubinin–Radushkevich (D–R) isotherm models very well. The constants values for the adsorption intensity of Freundlich; $1/n$ was found 0.49 and value of E implies Pb^{2+}-picrate adsorbed favorably and chemically on to the surface of resin (**1**).

Table 4
Langmuir, Freundlich and D–R characteristic constants for Pb^{2+}-picrate.

Langmuir				Freundlich			D–R		
Q	b	R_L	R^2	A	1/n	R^2	X_m	E	R^2
mmol/ g	mol/L 1×10^4			mol/g			mol/g	kJ/mol	
84.80	6.22	0.04–0.13	0.97	5.81×10^{-10}	0.49	0.99	635.17	11.62	0.99

4. Conclusion

The present study highlights the adsorption of especially Pb^{2+} from aqueous media onto resin (**1**). The results show that resin (**1**) is an effective and selective adsorbent for Pb^{2+} under optimized conditions. From kinetic study models the experimental data follow pseudo-second order equation. This adsorption process is thermodynamically favorable, spontaneous and endothermic in nature.

Acknowledgement

We are highly thankful to National Centre of Excellence in Analytical Chemistry, University of Sindh, for financial support.

References

[1] J.R. Rangel-mendez, M. Streat, Mercury and cadmium sorption performance of a fibrous ion exchanger and granular activated carbon, Process. Saf. Environ. Prot. 80 (2002) 150–158.
[2] K. Jia, B.C. Pan, Q.R. Zhang, X.S. Wang, B.J. Pan, W.M. Zhang, L. Lv, Impregnating titanium phosphate nanoparticles onto a porous cation exchanger for enhanced lead removal from waters, J. Colloid Interf. Sci. 331 (2009) 453–457.
[3] S. Tangjuank, N. Insuk, J. Tontrakoon, V. Udeye, World Academy of Science, Eng. Techn. 52 (2009) 110–116.
[4] M. Gaverilescue, Removal of heavy metal ions from environment by Biosorption, Eng. Life. Sci. 4 (2004) 219–232.
[5] M. Iqbal, R.G.J. Edyvean, Biosorption of lead, copper and zinc ions on loofa sponge immobilized biomass of Phanerochaete chrysosporium, Miner. Eng. 17 (2004) 217–223.
[6] K.C. Sekhar, C.T. Kamalaa, N.S. Chary, A.R.K. Sastry, T.N. Raoa, M. Vairamani, Removal of lead from aqueous solutions using an immobilized biomaterial derived from a plant biomass, J. Hazard. Mater. 108 (2004) 111–117.
[7] A. Selatnia, A. Boukazoula, N. Kechid, M.Z. Bakhti, A. Chergui, Y. J Kerchich, Biosorption of lead(II) from aqueous solution by a bacterial dead Streptomyces rimosus biomass, Biochemical. Eng. 19 (2004) 127–135.
[8] Guidelines for drinking-water quality, third edition, vol. 1, Recommendations WHO, 2004.
[9] J. Zhu, J. Yang, B. Deng, Ethylenediamine-modified activated carbon for aqueous lead adsorption, Environ. Chem. Lett. 8 (2010) 277–282.
[10] F. Boudrahem, F. Aissani-Benissad, A. Soualah, Adsorption of lead(II) from aqueous solution by using leaves of date trees as an adsorbent, J. Chem. Eng. Data 56 (2011) 804–1812.
[11] V. Numan Bulut, A. Gundogdub, C. Duran, H.B. Senturk, M. Soylak, L. Elci, M. Tufekci, A multi-element solid-phase extraction method for trace metals determination in environmental samples on Amberlite XAD-2000, J. Hazard Mater. 146 (2007) 155–163.
[12] M. Tuzen, M. Soylak, Column system using diaion HP-2MG for determination of some metal ions by flame atomic absorption spectrometry, Anal. Chim. Acta 504 (2004) 325–334.
[13] D. Mendil, M. Tuzen, M. Soylak, A biosorption system for metal ions on *Penicillium italicum* – loaded on Sepabeads SP 70 prior to flame atomic absorption spectrometric determinations, J. Hazard. Mater. 152 (2008) 1171–1178.
[14] I.B. Solangi, S. Memon, M.I. Bhanger, Synthesis and application of a highly efficient tetraester calix[4]arene based resin for the removal of Pb^{2+} from aqueous environment, Anal. Chim. Acta 638 (2009) 146–153.
[15] F.T. Minhas, I.B. Solangi, S. Memon, M.I. Bhanger, Kinetic study of an effective Pb(II) transport through a bulk liquid membrane containing calix[6]arene hexaester derivative as a carrier, Sep. Sci. Techn. 45 (2010) 1448–1455.
[16] Z. Xiaowei, J. Qiong, S. Naizhong, Z. Weihong, Yusheng Adsorption of Pb(II) from an aqueous solution by titanium dioxide/carbon nanotube nanocomposites: Kinetics, thermodynamics and isotherms, J. Chem. Eng. Data 55 (2010) 4428–4433.
[17] V.K. Gupta, Sorption dynamics, process development, and column operations for the removal of copper and nickel from aqueous solution and wastewater using activated slag, a low-cost adsorbent, Ind. Eng. Chem. Res. 37 (1998) 192–202.
[18] P. Yin, Q. Xu, R. Qu, G. Zhao, Y. Sun, Adsorption of transition metal ions from aqueous solutions onto a novel silica gel matrix inorganic-organic composite material, J. Hazard. Mater. 173 (2010) 710–716.
[19] R. Liu, P. Liang, Determination of trace lead in water samples by graphite furnace atomic absorption spectrometry after preconcentration with nanometer titanium dioxide immobilized on silica gel, J. Hazard. Mater. 152 (2008) 166–171.
[20] Q. He, Z. Hu, Y. Jiang, X. Chang, Z. Tu, L. Zhang, Preconcentration of Cu(II), Fe(III) and Pb(II) with 2-((2 aminoethylamino)methyl)phenol-functionalized activated carbon followed by ICP-OES determination, J. Hazard. Mater. 175 (2010) 710–714.
[21] V.S. Munagapati, V. Yarramuthi, S.K. Nadavala, S.R. Alla, K. Abburi, Biosorption of Cu(II), Cd(II) and Pb(II) by Acacia leucocephala bark powder: Kinetics, equilibrium and thermodynamics, Chem. Eng. J. 157 (2010) 357–365.
[22] M.E. Mahmoud, M.M. Osman, O.F. Hafez, E. Elmelegy, Removal and preconcentration of lead (II), copper (II), chromium (III) and iron (III) from wastewaters by surface developed alumina adsorbents with immobilized 1-nitroso-2-naphthol, J. Hazard. Mater. 173 (2010) 349–357.
[23] V. Tharanitharan, K. Srinivasan, Kinetic and equilibrium studies of removal of Pb(II) and Cd(II) ions from aqueous solution by modified duolite XAD-761 resins, Asian J. Chem. 22 (2010) 3036–3046.
[24] C.D. Gutsche, Calixarenes: Revisited, Royal Society of Chemistry, Cambridge, 1998.
[25] V. Böhmer, Calixarenes, macrocycles with (almost) unlimited possibilities, Angew, Chem. Int. Ed. Engl. 34 (1995) 713–775.
[26] A. Ikeda, S. Shinkai, Novel cavity design using calix[n]arene skeletons: Toward molecular recognition and metal binding, Chem. Rev. 97 (1997) 1713–1734.
[27] M. Yilmaz, Solution state metal complexes of calixarenes and polymeric calixarenes, in: N.P. Cheremisinoff (Ed.), Handbook of Engineering Polymeric Materials, Marcel Dekker, New York, NY, 1997, p. 339.
[28] S. Memon, G. Uysal, M. Yilmaz, Selective complexation of Hg^{2+} by biscalix[4]arene nitriles, Sep. Sci. Techn. 35 (2000) 1247–1256.
[29] G. Uysal, S. Memon, M. Yilmaz, Synthesis and binding properties of polymeric calix[4]arene Nitriles, React. Funct. Polym. 50 (2001) 77–84.
[30] S. Memon, M. Tabakci, D.M. Roundhill, M. Yilmaz, Useful approach toward the synthesis and metal extractions with polymer appended thioalkyl calix[4]arene, Polymers 46 (2005) 1553–1560.
[31] S. Erden, A. Demirel, S. Memon, M. Yilmaz, E. Canel, E. Kilic, Using of hydrogen ion-selective poly(vinyl chloride) membrane electrode based on calix[4]arene as thiocyanate ion-selective electrode, Sensor. Actu. B 113 (2006) 113–290.
[32] S. Memon, M. Tabakci, D.M. Roundhill, M. Yilmaz, Synthesis and evaluation of the Cr(VI) extraction ability of amino/nitrile calix[4]arenes immobilized onto a polymeric backbone, React. Funct. Polym. 66 (2006) 1342–1349.
[33] A. Yilmaz, S. Memon, M. Yilmaz, Synthesis and binding properties of calix[4]arene telomers, J. Polym. Sci. Part A: Polym. Chem. 37 (1999) 4351–4355.
[34] S. Memon, G. Uysal, M. Yilmaz, Synthesis and complexation studies of p-tert-butylcalix[4]crown telomers, J. Mac. Sci – Pure Appl. Chem. Part A. 38 (2001) 173–184.

[35] S. Memon, E. Akceylan, B. Sap, M. Tabakci, D.M. Roundhill, M. Yilmaz, Polymer supported calix[4]arene derivatives for the extraction of metals and dichromate anions, J. Poly. Env. 11 (2003) 67–74.
[36] M. Tabakci, S. Memon, B. Sap, D.M. Roundhill, M. Yilmaz, A calix[4]arene derived dibenzonitrile receptor modified at Its "Lower Rim" by a polymerizable group, J. Mac. Sci – Pure Appl. Chem. Part A 41 (2004) 811–825.
[37] S. Memon, O. Oğuz, A. Yilmaz, M. Tabakci, M. Yilmaz, Ş. Ertul, Synthesis and extraction study of calix[4]arene dinitrile derivatives incorporated in a polymeric backbone with bisphenol-A, J. Pol. Env. 9 (2001) 97–101.
[38] I.B. Solangi, S. Memon, N. Memon, M.I. Bhanger, Exploration of Pb^{2+} selective behavior of calix[6]arene ester derivatives, J. Mol. Sci Part-A. Pure Appl. Chem. 45 (2008) 1050–1010.
[39] D.M. Roundhill, I.B. Solangi, S. Memon, M.I. Bhanger, M. Yilmaz, The liquid–liquid extraction of toxic metals (Cd, Hg and Pb) by calixarenes, Pak. J. Anal. Env. Chem. 10 (2009) 1–13.
[40] A.T. Yordanov, B.R. Whittlesey, D.M. Roundhill, Calixarenes derivatized with sulfur-containing functionalities as selective extractants for heavy and precious metal Ions, Inorg. Chem. 37 (1998) 3526–3531.
[41] M. Tabachi, S. Memon, M. Yilmaz, D.M. Roundhil, Oligomeric calix[4]arene-thiacrown ether for toxic heavy metals, J. Pol. Sci Part A: Poly. Chem. 42 (2004) 186–193.
[42] I.B. Solangi, A.A. Bhatti, M.A. Kamboh, S. Memon, M.I. Bhanger, Comparative fluoride sorption study of new calix[4] arene-based resins, Desalination 272 (2011) 98–106.
[43] S. Memon, M. Yilmaz, Solvent extraction of metal cations by chemically modified biscalix[4]arenas, Sep. Sci. Tech. 36 (2001) 473–486.
[44] N. Kannan, T. Veemaraj, Removal of lead(II) ions by adsorption onto bamboo dust and commercial activated carbons—A comparative study, E. J. Chem. 6 (2009) 247–256.
[45] M. Kumar, D.P.S. Rathorea, A.K. Singh, Metal ion enrichment with Amberlite XAD-2 functionalized with Tiron: analytical applications, Analyst 125 (2000) 1221–1226.
[46] H.Z. Mousavi, B.A. Esfahanib, A. Arjmandi, Solid phase extraction of lead(II) by sorption on grinded eucalyptus stem and determination with flame atomic absorption spectrometry, J. Chin. Chem. Soc. 56 (2009) 974–980.
[47] F. Boudrahem, F.A. Benissad, A. Soualah, Adsorption of lead (II) from aqueous solution by using leaves of date trees as an adsorbent, J. Chem. Eng. Data 56 (2011) 1804–1812.
[48] Z.H. Huang, X. Zheng, L.W.M. Wang, Q.H. Yang, F. Kang, Adsorption of lead(II) ions from aqueous solution on low-temperature exfoliated graphene nanosheets, Langmuir 27 (2011) 7558–7562.
[49] S. Tangjuank, N. Insuk, J. Tontrakoon, V. Udeye, Adsorption of lead(II) and cadmium(II) ions from aqueous solutions by adsorption on activated carbon prepared from cashew nut shells, World Acad. Science Eng. Techn. 52 (2009) 1–7.
[50] M. Immamuglu, O. Tekir, Removal of copper (II) and lead (II) ions from aqueous solutions by adsorption on activated carbon from a new precursor hazelnut husks, Desalination 228 (2008) 108–113.
[51] X. Zhao, Q. Jia, N. Song, W. Zhou, Y. Li, Adsorption of Pb(II) from an aqueous solution by titanium dioxide/carbon nanotube nanocomposites: Kinetics, thermodynamics, and isotherms, J. Chem. Eng. Data 55 (2010) 4428–4433.
[52] E. Haribabua, Y.D. Upadhyaa, S.N. Upadhyaya, Removal of phenols from effluents by fly ash, Inter. J. Env. Stud. 43 (1993) 169–176.
[53] Y.S. Ho, G. McKay, Pseudo-second order model for sorption processes, Proc. Biochem. 34 (1999) 451–465.
[54] D. Reichenberg, Properties of ion-exchange resins in relation to their structure. III. Kinetics of exchange, J. Am. Chem. Soc. 75 (1953) 589–597.
[55] W.J. Morris, C. Weber, Kinetics of adsorption on carbon from solutions, J. Sanit. Eng. Div. ASCE 89 (1963) 31–59.
[56] G.Z. Memon, M.I. Bhanger, M. Akhtar, F.N. Talpur, J.R. Memon, Adsorption of methyl parathion pesticide from water using watermelon peels as a low cost adsorbent, Chem. Eng. J. 138 (2008) 616–621.
[57] A. Sari, D. Mendil, M. Tuzen, M. Soylak, Biosorption of Cd (II) and Cr(III) from aqueous solution by moss (*Hylocomium splendens*) biomass: Equilibrium, kinetic and thermodynamic studies, Chem. Eng. J. 144 (2008) 1–9.
[58] M.A. Kamboh, I.B. Solangi, S.T.H. Sherazi, S. Memon, Sorption of congo red onto p-tert-butylcalix[4]arene based silica resin, J. Iran. Chem. Soc. 8 (2011) 272–279.